



Event
Horizon
Telescope

Event Horizon Telescope
Memo Series

EHT Memo 2019-CE-01

Calibration & Error Analysis WG

Flux Density Calibration of the EHT Array

M. Janssen¹, L. Blackburn², S. Issaoun¹, T. P. Krichbaum³, M. Wielgus^{2,4}

April 07, 2019 – Version 1.0

¹*Department of Astrophysics/IMAPP, Radboud University Nijmegen, PO Box 9010, 6500 GL Nijmegen, The Netherlands*

²*Center for Astrophysics | Harvard & Smithsonian, 60 Garden St., Cambridge, MA 02138, USA*

³*Max Planck Institut für Radioastronomie (MPIfR), Auf dem Hügel 69, 53121 Bonn, Germany*

⁴*Black Hole Initiative at Harvard University, 20 Garden St., Cambridge, MA 02138, USA*

Abstract

This work summarizes the flux density calibration techniques developed for the EHT array and gives an overview of the derived station parameters used to calibrate the data of the first scientific data release of the 2017 EHT array. Special care is taken to accurately describe the uncertainties of the calibration process.

Contents

1 Principles of VLBI Amplitude Calibration	2
2 Telescope Parameters	3
2.1 System Temperatures	3
2.2 DPFUs and Gain Curves	5
2.3 Post-Processing	9
3 ANTAB Data Format	10
4 Flux Density Calibration Tools	11
5 Summary	12

1 Principles of VLBI Amplitude Calibration

By forming cross-correlations of recorded voltages from pairs of stations, a correlator measures signal-to-noise ratios (SNRs). A flux-scaling to a known brightness of a calibrator source is generally not possible because long baselines resolve most sources. Instead, known station sensitivities can be used to convert correlation coefficients to a physical flux density scale in units of Jansky (Jy). Sensitivities are given as system equivalent flux densities (SEFDs), which are formally defined as the measured flux density of an unresolved source within a telescope’s beam that would double the total system noise. In practice, the SEFD can be decomposed into different constituents, which describe separate aspects of the overall sensitivity of a telescope and are often measured in distinct ways:

- The system noise temperature T_{sys} [K] measures the sum of all noise contributions (the source itself, sky noise, receiver noise, etc.) along the signal path. For high frequency observations, an additional correction for the atmospheric opacity τ should be included in the SEFD to recover the true brightness of the observed astronomical source. Typically, this is done by using an **effective system temperature** $T_{\text{sys}}^* \equiv T_{\text{sys}} \exp(\tau)$. All 2017 EHT stations measure T_{sys}^* directly with the chopper-wheel method (Penzias & Burrus, 1973; Ulich & Haas, 1976). T_{sys}^* values are measured directly at a high cadence during an observation, by placing a calibration load with a known temperature in the signal path.
- The effective dish diameter A_{eff} , which is the physical dish diameter multiplied by an aperture efficiency factor $0 < \eta_A < 1$. The η_A efficiency would be unity for a perfect telescope dish. A_{eff} describes the effective collecting area of a dish after taking into account all possible losses and inefficiencies. These include the smoothness of the dish, under-illumination, blockage, and spill-over effects, and misalignments along the optics. A_{eff} describes the gain of a telescope at an optimal elevation, i.e., without elevation-dependent losses, which are discussed below. Usually, the optimal gain is measured and given as a **degrees per flux density unit (DPFU)** factor, to convert a measured system temperature in Kelvin into a flux density in Jy. The Boltzmann constant $k_B = 1.38 \times 10^{-23}$ J/K = 1.38×10^3 Jy/K relates the DPFU to the effective collecting area as $\text{DPFU} = A_{\text{eff}} / (2k_B)$. While elevation-dependent effects are factored out of the DPFU, time-dependent variations can occur, e.g., due to different dish characteristics during local day and night time. Stations’ DPFUs are determined from separate measurements of calibrator sources (planets typically) and parametrized as a function of time (t).
- The **gain curve (gc)** describes relative variations of the DPFU as a function of elevation, due to non-atmospheric effects (e.g., the deformation of a dish under its own weight). Gain curves are determined from observations of calibrator sources over a wide range of elevation. They are parametrized as a function of elevation (E) when used to calibrate visibilities.

- The **phasing efficiency** η_{ph} for phased-up connected-element interferometers describes the loss of sensitivity due to imperfect phase alignments between the individual stations. In the absence of phase errors, η_{ph} would be unity and the effective collecting area would be exactly equal to the sum of the individual collecting areas of all dishes. Formally, η_{ph} could be included in η_{A} . This is not done here, because the rapidly-varying phasing efficiency is fundamentally different from the usually constant mechanical efficiency factors that enter in η_{A} . Phasing efficiencies are determined directly from the measured interferometer visibilities during scans.

With these quantities, a station’s SEFD can be computed as

$$\text{SEFD} = \frac{1}{\eta_{\text{ph}}} \frac{T_{\text{sys}}^*}{\text{DPFU}(t) \text{gc}(E)}. \quad (1)$$

In this description, η_{ph} will be unity for single-dish stations. Finally, correlation coefficients $r_{i,j}$ formed from the recorded voltages of two stations i and j are ‘flux-calibrated’ via

$$r_{i,j} \rightarrow \sqrt{\text{SEFD}_i \text{SEFD}_j} r_{i,j}. \quad (2)$$

The cadence of T_{sys}^* and η_{ph} measurements determines the cadence of SEFD measurements. Within each scan, linear interpolation between measurements and constant extrapolation outside of the range of measured SEFDs should be used to fill the gaps and calibrate all visibilities. The SEFDs are usually stored in the ANTAB data format (Section 3).

2 Telescope Parameters

This section describes the methods used to determine telescope calibration parameters and the uncertainties in these parameters, with a special emphasis on the calibration of the 2017 EHT observing run. The numbers and uncertainties given are used for the calibration of the first scientific data release (SR1) from the 2017 EHT observations (EHT Collaboration et al., 2019b). Section 2.1 describes system temperatures, Section 2.2 presents DPFOs and gain curves, and Section 2.3 outlines post-processing methods of derived calibration parameters.

2.1 System Temperatures

For the 2017 EHT observations, different stations provided T_{sys}^* measurements in different formats. In the future, the VLBImonitor (EHT Collaboration et al., 2019a) will be used to query system temperatures in a unified format. In this section, site-by-site specifics about system temperature measurements are given. It should be noted that uncertainties in T_{sys}^* measurements are usually insignificant for the overall SEFD error budget (Issaoun et al., 2017a).

2.1.1 ALMA

The ALMA phasing project (Matthews et al., 2018) enables the inclusion of ALMA as a single phased-up station into the EHT array. The PolConvert (Martí-Vidal et al., 2016) software is used to convert the linear polarization signals measured by ALMA into a circular polarization basis measured by all other EHT stations. All flux density calibration parameters are generated by the QA2 analysis team (Goddi et al., 2019). Here, we briefly summarize this process.

Each ALMA dish measures system temperatures individually. These could be used to compute the overall SEFD of the full array, when η_{ph} is taken into account. However, it was found that bootstrapping sensitivities from self-calibration solutions of the array is a more reliable method to directly estimate SEFDs, to not bias the unweighted phased sum and because of

potentially erroneous T_{sys}^* measurements of individual stations. Instead, self-calibration Jones matrix gains are obtained for each 1.875 GHz ALMA spectral window and each ALMA sub-scan (~ 18 s). PolConvert then interpolates these gains to the correlator resolution of the EHT ($0.4 \text{ s} \times 58 \text{ MHz}$). The original self-calibration gains and measured effective system temperatures are available for cross-validation. The overall systematic uncertainty of the SEFDs is estimated to be around 10 %, based on the uncertainties of the flux density calibrator sources' brightness. Since self-calibration can wipe out intrinsic source variability, a slightly different calibration strategy will be employed for future EHT data releases, particularly for Sagittarius A*.

2.1.2 APEX

APEX uses the VLBI field system to provide T_{sys}^* values. The cadence is one measurement per scan. It was necessary to duplicate all system temperature values with ± 2 minute offsets with respect to the original time stamps, since the values were measured shortly before or after VLBI scans. This method guarantees that each T_{sys}^* measurement falls within the scan time of one VLBI scan. The gaps between two VLBI scans were always larger than two minutes plus the offset of the original T_{sys}^* time stamps from the start or end of a scan.

2.1.3 IRAM 30m

T_{sys}^* values from operator scan logs are used for the IRAM 30m telescope. The cadence is one value per scan.

2.1.4 JCMT

T_{sys}^* values from operator scan logs are used for the JCMT, corrected for a measured sideband ratio of 1.25 (<https://www.eaobservatory.org/jcmt/instrumentation/heterodyne/rxa/>).

2.1.5 LMT

The LMT records the measured total power in an independent data stream. This is used to track intra-scan T_{sys}^* variations with a 1 s cadence. The association to RCP and LCP of the recorded total power was verified by comparing its power spectrum to the power spectrum of the measured auto-correlations after the VLBI data correlation. A sideband ratio of unity is used for the double-sideband receiving system of the LMT. This ratio was not directly measured, but the mixers used at the LMT have been thoroughly characterized at the CARMA station to which it used to belong. The tests showed that the true sideband ratio is indeed very close to unity, well within the overall SEFD error budget for the LMT.

2.1.6 SMA

A phased array T_{sys}^* value is determined from the individual effective system temperature measurements (\mathcal{T}_i^*) of N phased-up stations as

$$T_{\text{sys}}^* = \left(\sum_{i=1}^N \frac{1}{\mathcal{T}_i^*} \right)^{-1}. \quad (3)$$

Phasing efficiencies are determined following [Young et al. \(2016\)](#) at a cadence of 10 s. η_{ph} is accurate to within 5–15 %, depending on the SNR of the interferometer data. A sideband ratio of unity is used for SMA's double-sideband system.

2.1.7 SMT

T_{sys}^* values from operator scan logs are used for the SMT. The cadence is one value per scan.

2.1.8 SPT

The SPT hot load calibration is done with the R2DBE. Therefore, separate T_{sys}^* values are estimated for the EHT low and high band in 2017. The nominal cadence is one system temperature measurement per scan.

2.2 DPFUs and Gain Curves

DPFUs and gain curves are estimated from measurements of the effective antenna temperature T_A^* of bright calibrator sources. T_A^* describes the opacity-corrected contribution of the observed source to the power measured by a telescope. Gain curves are typically determined by tracking bright, non-variable radio sources over a wide range of elevation. Usually, the following steps are taken:

1. The T_A^* data for several calibrators tracked over a sufficiently large range in elevation is gathered.
2. For each calibrator, the average over a small plateau range in elevation is used to normalize the data.
3. Obvious outliers from bad measurements should be removed.
4. The function $gc(E) = 1 - B \times (E - E_0)^2$ is fit to the data of all calibrators combined with a least-squares method. The chosen $gc(E)$ function ensures that the gain curve only describes changes relative to the DPFU. Uncertainties in the B and E_0 parameters are taken from the covariance matrix of the fit.

Observations of planets are typically used to compute a station's DPFU as

$$\text{DPFU} = \frac{T_A^*}{S_{\text{planet}}}, \quad (4)$$

with S_{planet} the in-beam flux density in Jy of the measured planet, computed with a model like GILDAS or the ALMA planet model.¹ In practice, the average T_A^* value from multiple measurements is taken. The measurements should be divided by the station's gain curve if scans at a non-optimal elevation are used. The uncertainty of the DPFU follows by adding the uncertainties from the measurement spread and the uncertainty in the value of S_{planet} provided by the model.² For SR1 data, the GILDAS planet model was used to estimate S_{planet} , with an added systematic uncertainty of 10%. The more recent ALMA planet model should be used for future data releases, since it is more accurate and has a well defined error budget. Usually, DPFUs are determined separately for the RCP and LCP receivers since they can have different sensitivities.

Uncertainties in the DPFU and the gain curve are the dominant contributions to the overall error budget of the SEFD, with the DPFU uncertainty usually being significantly larger than the gain curve uncertainty. Due to the parametrization of the gain curve, the error propagation makes the SEFD uncertainty a function of elevation. The error budget is largest at the most extreme elevations.

¹ See <http://www.iram.fr/IRAMFR/GILDAS/> and <https://library.nrao.edu/public/memos/alma/memo594.pdf>.

² If T_A^* values are measured by cross-scans, it is possible to assign an uncertainty to each individual T_A^* measurement, by fitting a Gaussian to the data. These uncertainties are taken into account. No scans at extreme elevations should be used, so the small gain curve uncertainties can be neglected.

2.2.1 ALMA

ALMA determines SEFDs directly based on self-calibration cycles (Section 2.1). For the EHT ANTAB tables, an average DPFU value of 0.031 K/Jy corresponding to a single 12 m dish is factored out of the SEFD estimates and a flat gain curve is used. The increase in sensitivity due to the total number of stations in the phased sum is therefore incorporated into the system temperature values in the EHT ANTAB tables. Any real gain curve variations are solved indirectly by the self-calibration.

2.2.2 APEX

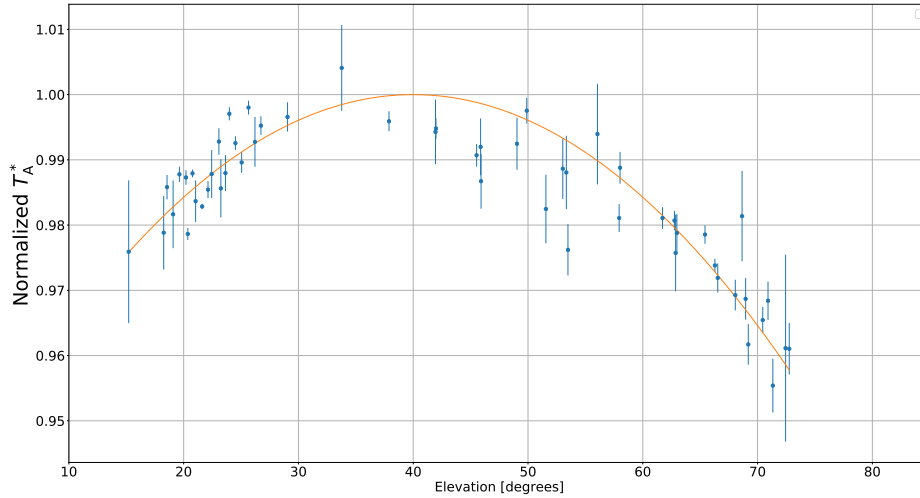


Figure 1: The APEX gain curve used for the EHT SR1 data calibration.

The DPFU was determined from scans on Saturn and Jupiter. The error due to intrinsic T_A^* measurement spread was 5%. Adding the uncertainty from the assumed planet model, a final error budget of 11% is obtained. Figure 1 shows the measured APEX gain curve from scans on Jupiter. The deviation from a flat gain curve is very small, at a level of only a few percent at the most extreme elevations. The uncertainties in the determined parameters are 3.6% and 1.0% for B and E_0 , respectively.

2.2.3 IRAM 30m

The DPFU was determined from scans on Saturn with an estimated overall uncertainty of 10%. Scans on 3C279, 3C273, and OJ287 were used to estimate the gain elevation dependence, shown in Figure 2. The uncertainties in the determined parameters are 5.3% and 1.3% for B and E_0 , respectively.

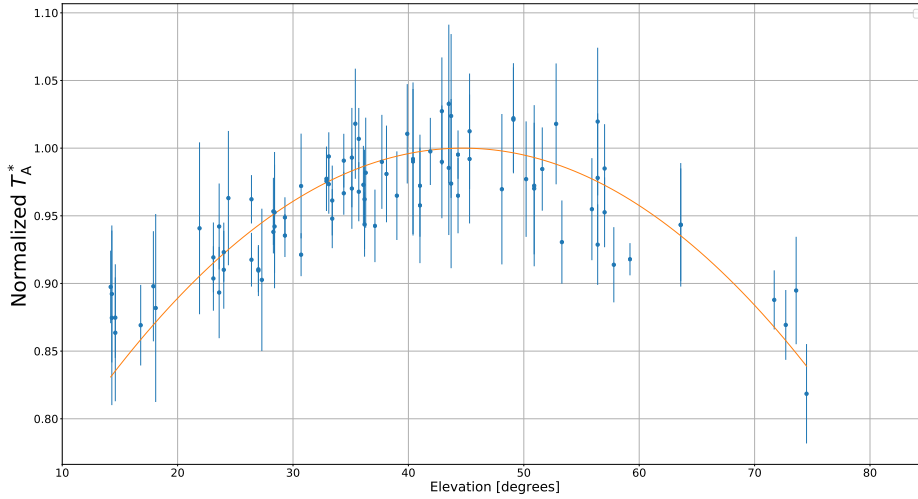


Figure 2: The IRAM 30m gain curve used for the EHT SR1 data calibration.

2.2.4 JCMT

Using historic planetary aperture efficiency measurements from 2006 to 2017, a clear time-dependent DPFU was derived for the JCMT, which is shown in Figure 3. During local (HST) night time, the DPFU is a constant, but during local day time, a clear drop in aperture efficiency is seen, as a result of thermal dish deformation induced by solar irradiation. In the EHT ANTAB tables, the time dependence of the aperture efficiency has been accounted for by replacing all T_{sys}^* measurements with $T_{\text{sys}}^*/\text{DPFU}(t)$ and setting the DPFU to unity in the header. The DPFU uncertainty is 10 % and 14 % during day and night time, respectively. The JCMT is the only EHT station where a time-dependent DPFU is supported by the calibrator data. Very sensitive continuum cameras monitoring the JCMT dish behaviour showed that the antenna does not display a gain-elevation dependence; so a flat gain curve is used for the EHT a priori calibration.

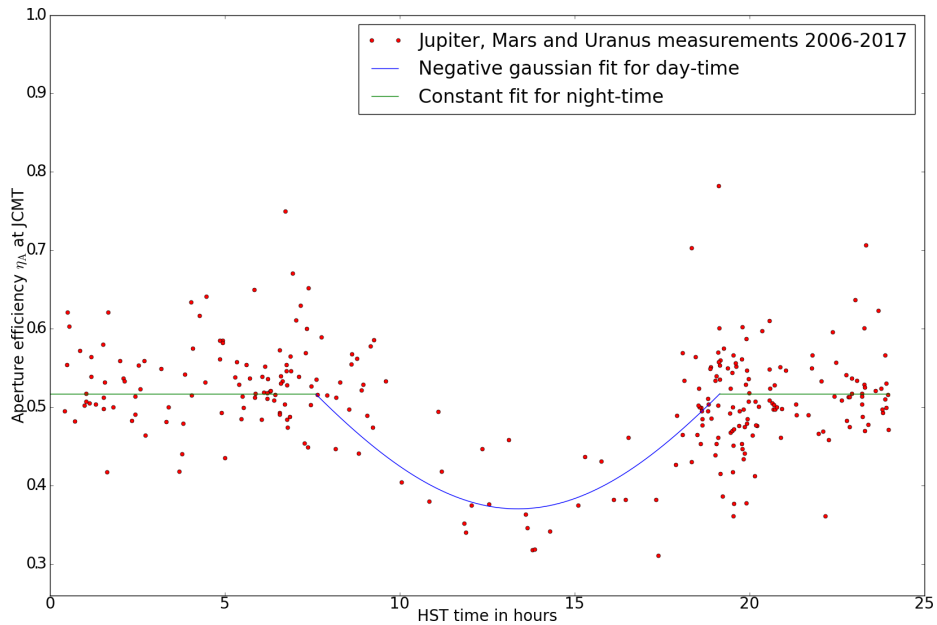


Figure 3: Local day and night time fits to the aperture efficiency of the JCMT (Issaoun et al., 2018).

2.2.5 LMT

The DPFU for the 32 m dish used during the 2017 EHT observations was determined from scans on Saturn at an optimal elevation, with an estimated overall uncertainty of 20 %. No concurrent data of sufficient quality was available to constrain the gain curve for the 2017 observations. While it is unclear how well the adaptive surface performs at extreme elevations for 230 GHz observations, a flat gain curve was assumed with a 10 % uncertainty, based on 2015 measurements with the AzTEC receiver.

With the installation of a chopper wheel, an accurate gain-elevation dependence for the new 50 m dish can be obtained with future calibrator observations.

2.2.6 SMA

The small 6 m dishes are well characterized. They have an aperture efficiency of 0.75, which is known to within 2 % based on holography measurements. Real-time focusing of the dishes, following a careful analysis of the antenna characteristics by [Matsushita et al. \(2006\)](#), eliminates the gain-elevation dependence. In the EHT ANTAB tables, the DPFU is set to unity and SEFDs are provided directly instead of T_{sys}^* values.

2.2.7 SMT

The SMT has been characterized in great detail by [Issaoun et al. \(2017b\)](#). The DPFU was determined based on Mars and Jupiter data with a 7 % uncertainty. Scans on the planetary nebula K3-50 and the star-forming region W75N were used to estimate the gain elevation dependence, shown in Figure 4. The uncertainties in the determined parameters are 10.4 % and 2.0 % for B and E_0 , respectively.

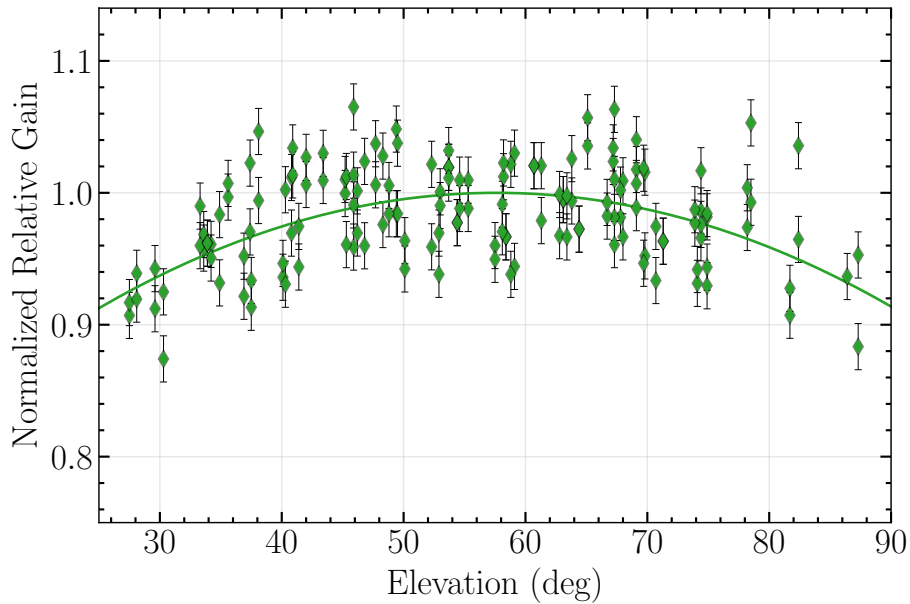


Figure 4: The SMT gain curve used for the EHT SR1 data calibration.

2.2.8 SPT³

The station DPFU was determined from scans on Saturn with an estimated overall uncertainty of 15 %. The special geographical situation of the SPT makes it impossible to track sources over ranges in elevation angle, since each source remains at constant elevation. Therefore, no gain curve could be determined for the SPT and a constant gain offset \mathcal{G}_s may be present for each observed source s . Given that the DPFU was determined from Saturn at an elevation of $E_0 = 22^\circ$, the gain errors are expected to scale as $\mathcal{G}_s \propto (E_s - E_0)^2$, for a source at a constant elevation of E_s . The 10 m SPT dish was under-illuminated to 6 m in 2017. For a small collecting area like this, the gain-elevation dependence is expected to be small.

2.3 Post-Processing

If there are known issues with the measured telescope metadata, or when known issues of station amplitudes not captured by the standard flux density calibration methods are to be corrected with ad-hoc factors, the ANTAB data should be post-processed before being applied to the data. For the SR1 data (EHT Collaboration et al., 2019b), the following corrections were applied:

- A frequency instability of the 17 year old IRAM 30m maser used in the 2017 observations was uncovered by examining the amplitude loss as a function of the correlator integration period, down to 2.048 ms.⁴ To correct for the resulting amplitude loss due to decoherence, the DPFU was scaled by 1/3.663. The defect maser has been replaced in 2018.
- The data recorded at APEX showed a small amplitude loss due to the presence of a one-pulse-per-second signal. This was corrected by scaling the DPFU with a 1/1.020 factor.
- Based on a study where the median difference in amplitudes between the RR and LL correlations were compared before and after the flux density calibration, it was found that the RCP and LCP T_{sys}^* values had to be swapped for APEX.
- SMA high band frequency channels in the 2017 data showed partial drop outs.⁵ For a fraction δ_v of channels without signal, the system temperatures are scaled by $(1 - \delta_v)^{-2}$. The following correction factors were applied to the 2017 high band SMA system temperatures:
 - 1.1378 from 00:00:00 to 03:05:00 UTC on April 05 to correct for 6.25 % missing bandwidth.
 - 1.5148 from 03:05:00 to 17:10:00 UTC on April 05 to correct for 18.75 % missing bandwidth.
 - 1.1378 from 04:50:00 to 15:00:00 UTC on April 06 to correct for 6.25 % missing bandwidth.
 - 1.1378 from 10:50:00 to 20:35:00 UTC on April 07 to correct for 6.25 % missing bandwidth.

³The SPT calibration information is based on an internal EHT notebook from Junhan Kim: <https://eventhorizontelescope.teamwork.com/#notebooks/99802>.

⁴ Coherence loss studies are summarized in two internal EHT memos from Vincent Fish and Mike Titus: <https://eht-wiki.haystack.mit.edu/api/deki/files/3849/=APEX-PV-ultrashort-APs.pdf> and <https://eventhorizontelescope.teamwork.com/#files/2051636>.

⁵ The SMA channel drop outs were characterized in an internal EHT notebook by Lindy Blackburn and André Young: <https://eventhorizontelescope.teamwork.com/#notebooks/114993?c=3979118>.

- At low SNR (e.g., low elevation scans), the SMA may measure spurious phasing efficiencies, resulting in unrealistically high estimates for the SEFDs. After a careful analysis of the variability in the amplitudes after applying the SMA SEFDs, it was found that the spurious SEFDs can be removed by a sliding median window filter, which clips values outside of a reasonable range. The following smoothing was done for both SMA high and low band:
 - From 01:14:12 to 01:42:00 UTC on April 10, clipping SEFDs > 100000 Jy.
 - From 04:44:34 to 05:00:00 UTC on April 11, clipping SEFDs > 15000 Jy.
 - From 05:15:00 to 05:52:00 UTC on April 11, clipping SEFDs > 10000 Jy.
 - From 05:55:00 to 07:00:00 UTC on April 11, clipping SEFDs > 10000 Jy.

More accurate phasing efficiencies can be obtained by a careful analysis of the SMA interferometric data.

3 ANTAB Data Format

The standard ANTAB format is used to store the flux density calibration parameters in an ASCII text format. A full description of the ANTAB format is given in <http://www.aips.nrao.edu/cgi-bin/ZXHLP2.PL?ANTAB>. Below, an overview of the basic formatting choices is given:

1) First, the *gain group* is given – a single line for each station, which lists the DPFU and gain curve:

```
GAIN <stationcode> <mount-type> DPFU = <G:rcp>, <G:lcp> POLY = <a0>, <a1>, <a2>, <a3>, ... /
```

Here, <mount-type> is typically ALTAZ, <G:rcp> and <G:lcp> are the DPFU values in [K/Jy] for the RCP and LCP receiver, respectively, and <a_i> are the polynomial coefficients of the gain curve. For the $gc(E)$ parametrization used in this memo (Section 2.2), we have $a_0 = 1 - BE_0^2$, $a_1 = 2BE_0$, $a_2 = -B$, and $a_3 = a_4 = a_5 = \dots = 0$.

2.1) Second, the *Tsys group* is listed, containing blocks of system temperatures with columns per spectral IF (or spectral window) and rows for the time spacing. For each station a block starts with

```
TSYS <stationcode> timeoff=<To> INDEX = 'i1', 'i2', 'i3', ... /
```

Where, the '*i_j*' assign columns to RCP, LCP and spectral IFs. The timeoff=<To> parameter is an optional keyword. If used, the timestamps of all system temperature values in this block are shifted by <To> seconds. This may be useful to shift the times of the measurements into the VLBI scan times.

2.2) Next, the Tsys values for the station block are given; one line for every timestamp:

```
<UT-day> <UT-time> <T1> <T2> <T3> ...
```

With <UT-day> in the ddd format, <UT-time> in a hh:mm.mm format, and <T_j> the T_{sys} values in Kelvin assigned by *i_j* to a receiver spectral IF.

2.3) Lastly, a station block is terminated with a / and the next one can start:

```
/
TSYS <next stationcode> INDEX = ... /
...
```

Below, an example of an ANTAB table is given. The DPFU and gc values shown are the ones that were ultimately applied to the EHT SR1 data. Dummy values are shown for the system temperature values and indices.

```
GAIN AA ELEV DPFU = 0.031 POLY = 1.0 /
GAIN AP ELEV DPFU = 0.02453, 0.02496 POLY = 0.979519, 0.00115059, -0.00001616 /
GAIN AZ ELEV DPFU = 0.01683, 0.01681 POLY = 0.727119, 0.00947339, -0.00008222 /
GAIN JC ELEV DPFU = 1.0 POLY = 1.0 /
GAIN LM ELEV DPFU = 0.0824, 0.0826 POLY = 1.0 /
GAIN PV ELEV DPFU = 0.0344, 0.0333 POLY = 0.658617, 0.0156168, -0.0001786 /
GAIN SM ELEV DPFU = 1.0 POLY = 1.0 /
GAIN SP ELEV DPFU = 0.006094 POLY = 1.0 /

TSYS PV INDEX = 'R2', 'L2', 'R1', 'L1' /
141 03:00.317 131.89 142.49 132.70 142.70
141 03:01.867 132.07 142.76 132.77 142.76
!... and so on (exclamation mark = comment char)
/
TSYS AZ INDEX = 'L1', 'L2', 'R1', 'R2' /
141 03:01.456 122.24 291.24 117.59 332.75
141 03:02.956 122.18 292.14 117.66 331.82
!... and so on
/
!... idem for the other station blocks
```

The system temperatures, DPFUs, and gain curves can be read from ANTAB files by VLBI data calibration software packages to form SEFDs and perform the amplitude calibration (Equation 2).

4 Flux Density Calibration Tools

The public git repository https://bitbucket.org/M_Janssen/eht-flux-calibration contains scripts that can be used for the flux density calibration methods described in this memo:

- Fitting of station gains.
- Read and parse system temperatures from telescope metadata.
- Post-processing and sanity-checks of ANTAB data.

The <https://github.com/sao-eh/eat> software package contains a generalized ANTAB table parser, which can flux-calibrate any UVFITS file and perform additional sanity checks of the ANTAB data. The eat toolkit was used for the a priori calibration of all SR1 data.

5 Summary

Table 1: Effective flux density calibration parameters for SR1. For phased arrays (ALMA and SMA), the DPFUs represent the sensitivity of all phased dishes. The gain curve parameters are given based on the $gc(E) = 1 - B \times (E - E_0)^2$ parametrization.

Station	RCP DPFU [K/Jy]	LCP DPFU [K/Jy]	B	E_0
ALMA ^a	$1.03 \pm 10\%$	$1.03 \pm 10\%$	0	0
APEX	$0.02453 \pm 11\%$	$0.02496 \pm 11\%$	$0.000016 \pm 3.6\%$	$36.6 \pm 1\%$
IRAM 30m	$0.0344 \pm 10\%$	$0.0333 \pm 10\%$	$0.000177 \pm 5.3\%$	$43.7 \pm 1.3\%$
JCMT ^b	$(0.026 \pm 14\%) - (0.033 \pm 11\%)$	$(0.026 \pm 14\%) - (0.033 \pm 11\%)$	0	0
LMT ^c	$0.0824 \pm 22\%$	$0.0826 \pm 22\%$	0	0
SMA ^d	$0.046 \pm (5 - 15)\%$	$0.046 \pm (5 - 15)\%$	0	0
SMT	$0.01683 \pm 7\%$	$0.01681 \pm 7\%$	$0.000082 \pm 10.4\%$	$57.6 \pm 2.0\%$
SPT ^e	$0.006094 \pm 15\%$	$0.006094 \pm 15\%$	0	0

^aThe ALMA DPFU uncertainty is based on the overall 10% uncertainty estimated by the QA2 team.

^bFor the JCMT DPFU, a range between the smallest day time value and the night time value is given.

^cThe LMT has an added unparametrized 10% uncertainty on the gain curve, that has been added to the DPFU uncertainty.

^dThe SMA DPFU uncertainty is based on the dominant 5-15% uncertainty on the phasing efficiency.

^eThe gain curve of the SPT is uncharacterized.

This memo outlines the flux density calibration techniques for the EHT array. A special emphasis is placed on the uncertainties associated with the flux density calibration process, which are often glossed over in other VLBI experiments. The derived uncertainties can be used to guide downstream analysis tools, by restricting self-calibration gains to reasonable ranges and by providing a weighting on the reliability of visibility amplitudes across the array. Table 1 provides an overview of the derived calibration parameters for the first scientific data release of the EHT (EHT Collaboration et al., 2019b). Note that these numbers represent the overall station sensitivities, but may differ from the actual numbers in the EHT ANTAB tables. For some stations, DPFUs are already factored into the T_{sys}^* values in the ANTAB tables for example.

References

- EHT Collaboration et al. 2019a, ApJL, 875, L2 (Paper II)
- EHT Collaboration et al. 2019b, ApJL, 875, L3 (Paper III)
- Goddi, C., Marti-Vidal, I., Messias, H., et al. 2019, arXiv e-prints, 1901.09987
- Issaoun, S., Falcke, H., Friberg, P., et al. 2018, EHT Memo Series, 2018-CE-01
- Issaoun, S., Folkers, T. W., Blackburn, L., et al. 2017a, EHT Memo Series, 2017-CE-02
- Issaoun, S., Folkers, T. W., Marrone, D. P., et al. 2017b, EHT Memo Series, 2017-CE-03
- Martí-Vidal, I., Roy, A., Conway, J., & Zensus, A. J. 2016, A&A, 587, A143
- Matsushita, S., Saito, M., Sakamoto, K., et al. 2006, in Proceedings of the SPIE, Vol. 6275, Society of Photo-Optical Instrumentation Engineers (SPIE) Conference Series, 62751W
- Matthews, L. D., Crew, G. B., Doeleman, S. S., et al. 2018, PASP, 130, 015002
- Penzias, A. A. & Burrus, C. A. 1973, ARA&A, 11, 51
- Ulich, B. L. & Haas, R. W. 1976, ApJS, 30, 247
- Young, A., Primiani, R., Weintroub, J., et al. 2016, in Phased Array Systems and Technology (ARRAY), 2016 IEEE International Symposium on, 18-21 Oct. 2016